Deep-Sea Research I 57 (2010) 319–327

Contents lists available at ScienceDirect

Deep-Sea Research I

journal homepage: www.elsevier.com/locate/dsri

Flux comparison of Eulerian and Lagrangian estimates of Agulhas leakage: A case study using a numerical model

Erik van Sebille [a,*,1], Peter Jan van Leeuwen [a,2], Arne Biastoch [b], Wilhelmus P.M. de Ruijter [a]

[a] Institute for Marine and Atmospheric Research Utrecht, Utrecht University, Netherlands
[b] Leibniz Institute of Marine Sciences, Kiel, Germany

ARTICLE INFO

Article history:
Received 30 June 2009
Received in revised form
10 December 2009
Accepted 27 December 2009
Available online 11 January 2010

Keywords:
Agulhas leakage
Numerical lagrangian drifters
Interocean exchange
Eddy formation
Model validation
Mooring array design

ABSTRACT

Estimating the magnitude of Agulhas leakage, the volume flux of water from the Indian to the Atlantic Ocean, is difficult because of the presence of other circulation systems in the Agulhas region. Indian Ocean water in the Atlantic Ocean is vigorously mixed and diluted in the Cape Basin. Eulerian integration methods, where the velocity field perpendicular to a section is integrated to yield a flux, have to be calibrated so that only the flux by Agulhas leakage is sampled. Two Eulerian methods for estimating the magnitude of Agulhas leakage are tested within a high-resolution two-way nested model with the goal to devise a mooring-based measurement strategy. At the GoodHope line, a section halfway through the Cape Basin, the integrated velocity perpendicular to that line is compared to the magnitude of Agulhas leakage as determined from the transport carried by numerical Lagrangian floats. In the first method, integration is limited to the flux of water warmer and more saline than specific threshold values. These threshold values are determined by maximizing the correlation with the float-determined time series. By using the threshold values, approximately half of the leakage can directly be measured. The total amount of Agulhas leakage can be estimated using a linear regression, within a 90% confidence band of 12 Sv. In the second method, a subregion of the GoodHope line is sought so that integration over that subregion yields an Eulerian flux as close to the float-determined leakage as possible. It appears that when integration is limited within the model to the upper 300 m of the water column within 900 km of the African coast the time series have the smallest root-mean-square difference. This method yields a root-mean-square error of only 5.2 Sv but the 90% confidence band of the estimate is 20 Sv. It is concluded that the optimum thermohaline threshold method leads to more accurate estimates even though the directly measured transport is a factor of two lower than the actual magnitude of Agulhas leakage in this model.

1. Introduction

The magnitude of Agulhas leakage, the flux of water in the Agulhas Current that ends up in the Atlantic Ocean, is related to the strength of the Atlantic meridional overturning circulation (Weijer et al., 1999; Knorr and Lohmann, 2003; Biastoch et al., 2008b, 2009b). That is why an accurate monitoring of the variability of Agulhas leakage may yield a precursor of northern Atlantic Ocean climate variability. The Agulhas leakage is not a steady flow of water from the Indian to the Atlantic Ocean, but is carried in mesoscale eddies (Agulhas rings and cyclones), filaments, and non-rotating patches (Gordon, 1986; Lutjeharms and Cooper, 1996; Doglioli et al., 2006; Van Sebille et al., 2010) that shed from the Agulhas Current retroflection south of Africa before drifting into the Atlantic Ocean, in the meantime deforming, splitting, and merging (Boebel et al., 2003).

The variability and intermittency of Agulhas leakage makes monitoring difficult, and estimates of even the mean amount of Agulhas leakage have a wide range (from 4 Sv (Schmitz, 1995) to 41 Sv (Speich et al., 2006)) although most estimates lie between 10 and 20 Sv (e.g. Gordon, 1986; Thompson et al., 1997; Garzoli and Goni, 2000; Doglioli et al., 2006; Richardson, 2007). One of the most widely used methods in models to estimate the magnitude of Agulhas leakage is based on integrating the modeled velocity over some vertical plane close to the Agulhas Current retroflection (e.g. Dijkstra and De Ruijter, 2001; Matano and Beier, 2003; Treguier et al., 2003; Reason et al., 2003; Hermes et al., 2007).

However, such Eulerian methods may not be very apt for determining the magnitude of Agulhas leakage. This is because the Agulhas Current retroflection and leakage are not the only circulation systems within the greater Agulhas region. Closely linked to the Agulhas Return Current is the Subtropical Front of

* Corresponding author. 4600 Rickenbacker Causeway, Miami, FL 33131, USA.
E-mail address: EvanSebille@rsmas.miami.edu (E. van Sebille).
[1] Now at the Rosenstiel School of Marine and Atmospheric Science, University of Miami, Miami, FL, USA.
[2] Now at the Department of Meteorology, University of Reading, UK.

0967-0637/$ - see front matter Published by Elsevier Ltd.
doi:10.1016/j.dsr.2009.12.006

the Antarctic Circumpolar Current and the Agulhas system is intruded in the west by the subtropical gyre of the southern Atlantic Ocean. The water carried by these two circulation systems is vigorously mixed with the Agulhas leakage in the Cape Basin (Boebel et al., 2003; Giulivi and Gordon, 2006). This mixing can complicate the Eulerian measurement of the magnitude of Agulhas leakage, as it may be unclear what fraction of a certain flux is Agulhas leakage water and what fraction is related to other sources (Gordon, 1986; Boebel et al., 2003; You et al., 2003). Nevertheless, the 10–20 Sv range in Eulerian estimates of the magnitude of Agulhas leakage in models seems to agree with estimates obtained by other methods.

The difficulty in determining the magnitude of Agulhas leakage arises because the Agulhas region is not enclosed by continental boundaries. For that reason the integration of Eulerian velocities cannot be performed on a section between two coasts, although the oceanic net flux in other regions of the world ocean can be measured in this way. Examples of arrays employing such methods are located in the Atlantic Ocean (Bryden et al., 2005), in the Mozambique Channel (Ridderinkhof et al., 2010), and in the straits of the Indonesian Archipelago (Gordon et al., 1999). In the Agulhas region, however, integration cannot be done on the section between South Africa and Antarctica, as the eastward flowing Antarctic Circumpolar Current will then dominate the signal (e.g. Ganachaud and Wunsch, 2000). This is one of the reasons why inverse modeling of Agulhas leakage is so difficult (Schmitz, 1995; Casal et al., 2009). Donners and Drijfhout (2004) have shown that inverse modeling might even be impossible for the Agulhas system, since there is an overlap in the density class of some of the Agulhas leakage and some of the Antarctic Circumpolar Current.

Because of these problems, a method is needed capable of indicating how and where to deploy a (virtual) mooring array in order to obtain a time series of fluxes that resembles the time series of the amount of Agulhas leakage closely. The GoodHope line (see Fig. 1) is a good location due to its proximity to the Agulhas Current retroflection, yet the flux of water that returns to the Indian Ocean after crossing the line is negligible (Van Sebille et al., 2010). The GoodHope line (Ansorge et al., 2005; Swart et al., 2008) has been used for estimating the magnitude of Agulhas leakage in the Benguela Source and Transport (BEST) and Agulhas-South Atlantic Thermohaline Transport Experiment (ASTTEX) programs (Byrne and McClean, 2008; Baker-Yeboah, 2008), where a series of pressure inverted echo sounders were deployed on the ocean floor. These instruments do not directly measure velocity, so in order to compute Eulerian fluxes an additional two-layer model has to be employed. Such a model was employed by Garzoli and Goni (2000), who have used measurements from the ASTTEX program to calibrate an altimetry-based method of estimating the flux in the thermocline fraction of Agulhas leakage.

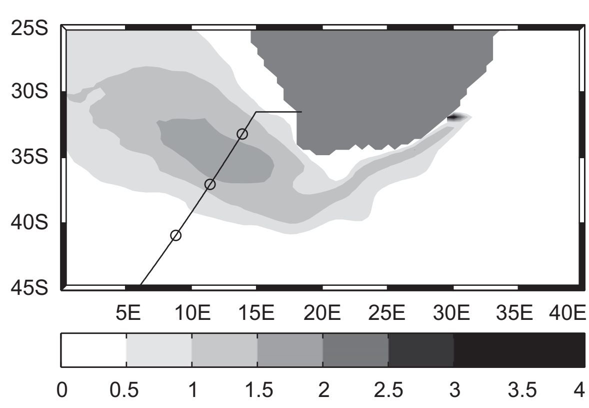

Fig. 1. The density of the numerical float trajectories for floats that end up in the Atlantic Ocean, in Sverdrup. The density is calculated on a $0.5^\circ \times 0.5^\circ$ grid. The thick black line in the Atlantic Ocean denotes the location of the GoodHope line, with the circles the positions of the 500, 1000, and 1500 km offshore points.

The approach used here is to limit the integration to only a subdomain of the entire GoodHope line. Two methods are discussed: One where the subdomain is bounded by the temperature and salinity of the water, and a second one where the subdomain is bounded by depth and offshore distance.

The first method (Section 4) is based on the thermohaline properties of Agulhas leakage. The thermocline water of the Indian Ocean at 450 m depth is typically 1 °C warmer and 0.1 g/kg more saline than the thermocline water of the Atlantic Ocean and Southern Ocean. In the case that the Agulhas leakage maintains these characteristics on its way through the Cape Basin, it should in principle be discriminated from the other water masses at the GoodHope line. Unfortunately, mixing in the Cape Basin is vigorous (Boebel et al., 2003) and the Agulhas rings in which most Agulhas leakage detaches from the Agulhas Current experience a fast decay (Byrne et al., 1995; Schouten et al., 2000). The Indian Ocean water will therefore be diluted once it reaches the GoodHope line. Nevertheless, it might be possible to capture part of the leakage in this way. Note that this method will only resolve the Agulhas leakage in the thermocline, as the Indian Ocean water below the thermocline does not differ very much from the water in the adjacent oceans (Van Aken et al., 2003). Such a water mass classification method for estimating the magnitude of Agulhas leakage was applied by Gordon et al. (1987), who came to an Agulhas leakage estimate of 10 Sv based on a comparison of the thermohaline characteristics of water in the southeast Cape Basin and in the Agulhas Current.

The second method (Section 5) is based on the location where Agulhas leakage crosses the GoodHope line. One can try to find an optimum Euclidean integration area: a rectangular area within which the integrated velocity is as close as possible to the time series of the flux of Agulhas leakage. The major problem with this method is that the shape of the area might be highly model-dependent, because it is an empirical method and neglects the dynamics of the Agulhas system.

2. The model

The two methods for confining the integration area are tested within the AG01 model (Biastoch et al., 2008b, 2008c), a two-way nested high-resolution model of the Agulhas region. This is a $1/10^\circ$ numerical ocean model of the Agulhas region (20°W-70°E; 47°S-7°S) based on the NEMO code (Madec, 2006, version 2.3). The model has 46 vertical layers, with layer thicknesses ranging from 6 m at the surface to 250 m at depth. The model employs partial cells at the ocean floor for a better representation of bathymetry.

The regional AG01 model is nested within a global model, ORCA, a $1/2^\circ$ global ocean–sea-ice model which is also based on NEMO. The two-way nesting allows for information exchange between the two models (Debreu et al., 2008). Not only are the boundary conditions of the high-resolution AG01 model taken from the low-resolution ORCA model, but the low-resolution ORCA model also gets updated by the high-resolution AG01 model at shared grid points. The Agulhas region dynamics is therefore affected by the global circulation, and vice versa. In this approach, the two models have to be run simultaneously. The two models are forced with the CORE data set of daily wind and surface forcing fields (Large and Yeager, 2004) for the period 1958–2004. The model is spun up for ten years, which leaves a 37 year time series at five day resolution (1968–2004) for Eulerian analysis.

The trajectories of the numerical Lagrangian floats are integrated using the ARIANE package (Blanke and Raynaud, 1997). Floats are released every five days in a 300 km zonal section of the Agulhas Current core at 32°S. The number of floats which are released at a particular moment is based on the transport per grid cell. Each float represents a certain transport, with a maximum of 0.1 Sv. Using the five day mean velocity fields, the floats are advected for a maximum of five years. When a float hits one of the trajectory boundaries, the integration of that float is stopped. These trajectory boundaries are at 32°S and 40°E in the Indian Ocean, at 47°S in the Southern Ocean, and at 5°S and 20°W in the Atlantic Ocean. The floats are advected with the flow, which means that they are not bound to a particular model layer. Biastoch et al. (2008b, 2008c) have used the same model and Lagrangian techniques to simulate Agulhas Current transport and Agulhas leakage.

In the 37 year period, 5.6×10^6 floats are released, which constitutes a mean Agulhas Current transport at 32°S of 64 Sv. On the five day resolution, however, the Agulhas Current strength ranges from 30 Sv to 128 Sv. As shown by Biastoch et al. (2009a), the strength of the Agulhas Current in the model is in agreement with over a year of in situ measurements by Bryden et al. (2005), who report an Agulhas Current range from 9 Sv to 121 Sv, with a mean of 70 Sv. After the five year integration period, only 3% of the numerical floats have not left the domain. The mean magnitude of Agulhas leakage in the model is 16.7 Sv, as measured over the GoodHope line. This is higher than the mean magnitude of Agulhas leakage in the study of Biastoch et al. (2008c) (12 Sv), which was based on the same model, because these authors used only the first four years of the float data set. As shown by Biastoch et al. (2009b), there is a positive trend in Agulhas leakage due to a southward shift of the subtropical front.

The AG01 model is the model that has been shown to be superior in a three-model quantitative skill assessment (Van Sebille et al., 2009b) and the model has been shown to accurately reproduce some of the key features in the Agulhas region (Biastoch et al., 2008a, 2008b, 2008c, 2009a). At the GoodHope line, the sea surface height variability in the model is comparable to that from the AVISO merged absolute dynamic topography data (Fig. 2). Since the model is not assimilative, it should not one-to-one be compared to satellite data. The agreement between sea surface height in the model and in the observations can be quantified using statistics of the patches defined by the 0.0 m isopleth, a first indication of Agulhas ring activity. The mean crossing locations of the patches found in the two data sets agree well (873 ± 124 km offshore for the model and 846 ± 143 km offshore for the observations) and the same is true for the mean width of the patches (585 ± 258 km for the model and 538 ± 290 km for the observations). Although all this suggests that the AG01 might be apt for studying Agulhas leakage over the GoodHope line, one should remember that this is a model-only study.

The magnitude of Agulhas leakage as determined from the numerical Lagrangian floats is taken here as the 'truth' time series F_{AL} and it is used for determining the skill of the Eulerian methods. Note that in this setup of the experiments the model is calibrated with itself. Therefore, it may be hard to translate the results of this study to the real ocean. Nevertheless, the results might serve as a first feasibility test for a monitoring program in the real ocean.

The velocity profile perpendicular to the GoodHope line can be measured as a function of time, either by using Acoustic Doppler Current Profilers (ADCPs), by using CTD sensors in combination with the thermal wind balance, or by using inverted echo sounders and reduced gravity models (Garzoli and Goni, 2000; Baker-Yeboah, 2008). In this study, we will deploy virtual current meters within the AG01 model. To mimic a mooring array, the velocity fields perpendicular to the GoodHope line are regridded to a resolution of 50 m in depth and 50 km in offshore distance. This particular resolution means that a velocity of $1\,\mathrm{m\,s^{-1}}$ in a certain grid cell results in a flux of 2.5 Sv. This flux can be either into the Atlantic Ocean (defined as positive), or into the Indian Ocean (defined as negative).

The location of each float crossings at the GoodHope line is determined using a three-dimensional linear interpolation. The temperature and salinity of the water at each of these crossing locations is determined by a two-dimensional interpolation of the (Eulerian) model temperature and salinity fields at the GoodHope line at the moment of float crossing. In this way the thermohaline

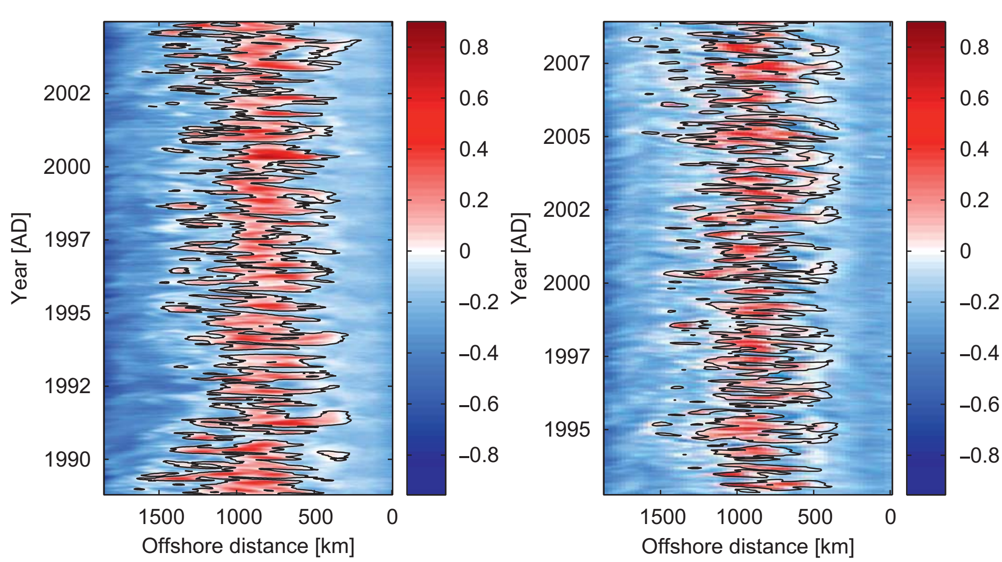

Fig. 2. Hovmoller diagrams of the sea surface height, in m, at the GoodHope line, from the model (left panel) and from altimetry data (right panel) on the same color scale. The altimetry data is taken from the merged absolute dynamic topography from the AVISO data center. The time series do not completely overlap, but are of the same length. The black lines are the 0.0 m isopleths, and are added to get an impression of Agulhas ring variability. Although there are some differences in the frequency, the mean location and width of the patches higher than 0.0 m in the model is comparable to these in the satellite data. (For interpretation of the references to color in this figure legend, the reader is referred to the web version of this article.)

properties of the Agulhas leakage can be determined. The results of this interpolation are relatively insensitive to the temporal resolution of the float release and model data (Van Sebille et al., 2009a).

Note that there seems to be a fundamental dichotomy related to the use of numerical Lagrangian floats for temperature and salinity analysis: The floats are allowed to mix heat and salt with their surrounding but at the same time it is assumed that all their transport originated in the Agulhas Current. This discrepancy, which turns out to be misleading and not true, is further discussed in Section 6.

3. Qualitatively comparing the flux profiles

When a composite of the mean Eulerian flux perpendicular to the GoodHope line is compared to the distribution of the transport by numerical Lagrangian float crossings through that line, the high agreement between the Eulerian and Lagrangian fields close to the coast and in the upper ocean is evident (Fig. 3, note that this depicts the mean profiles on the GoodHope line and individual rings and cyclones cannot be discerned). Apparently, the Agulhas leakage as sampled by the Lagrangian floats in the model is limited to the upper 1500 m, and reaches only 1200 km offshore. This is remarkable, as the Eulerian velocity profile does show significant transport deeper and more southward than this region.

There are two maxima in float crossing position. The first is in the region 500–1200 km offshore and is related to Agulhas rings, Agulhas cyclones, and filaments and other non-rotating features as a more thorough analysis of the trajectories reveals (not shown). In the Agulhas rings and cyclones, floats may cross the GoodHope line multiple times as they swirl inside the ring and this explains the bipolar structure in float crossing distribution. The distribution is asymmetric since these floats always cross the GoodHope line an odd number of times, as they are released in the Indian Ocean but end in the Atlantic Ocean. This eddy corridor is centered around 900 km offshore, which is at 12°E and 36°S. The second local maximum of float crossings is located within 200 km

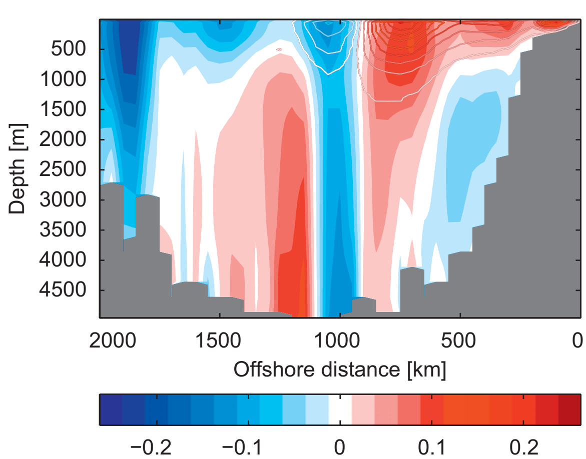

Fig. 3. The mean of the flux perpendicular to the GoodHope line (in Sverdrup per 50 m × 50 km grid cell) in the model run. See Fig. 1 for the location of the GoodHope line. Red colors denote a mean flux into the Atlantic Ocean while blue colors denote a mean flux into the Indian Ocean. The lines indicate the distribution of numerical float crossings (also in Sverdrup per 50 m × 50 km grid cell). The floats are released in the Agulhas Current over the entire water column. Note that for this distribution every crossing of a float is taken into account and that one float can cross the GoodHope line multiple times. The agreement between the velocity-integrated profile and the float transport is high in the upper 1000 m and until 1200 km offshore. (For interpretation of the references to color in this figure legend, the reader is referred to the web version of this article.)

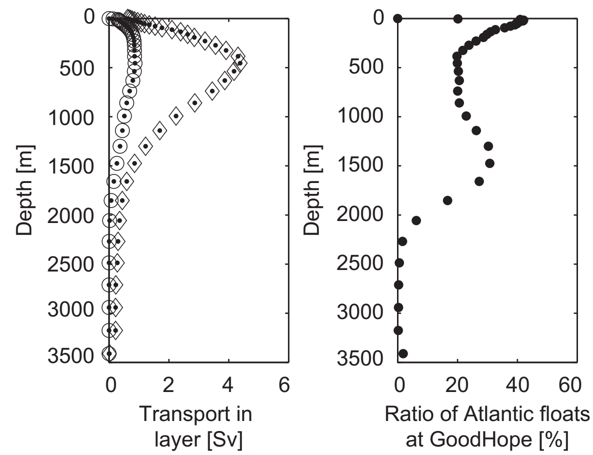

Fig. 4. The transport per model layer (left panel) for all floats when they are released in the Agulhas Current (diamonds), and for the floats that end in the Atlantic Ocean when they cross the GoodHope line (circles). The right panel shows the ratio of floats ending in the Atlantic Ocean as a function of model layer. While the Agulhas Current contains approximately 30% floats which end in the Atlantic Ocean in the upper 2000 m, this ratio reduces to almost zero below 2000 m.

of the African coast, on the continental slope. This core is probably related to the Good Hope Jet, a frontal boundary current feeding into the Benguela system (Bang and Andrews, 1974; Gordon et al., 1995).

Although the velocity profile at the GoodHope line has a large barotropic component, especially in the eddy corridor of maximum float crossing, the floats seem to be confined to the upper 1500 m. This despite the fact that there are floats which are released deeper in the Agulhas Current (Fig. 4). Apparently, only the upper part of the Agulhas Current leaks into the Atlantic Ocean and the lower part is returned into the Indian Ocean before crossing the GoodHope line in this model. The relative shallowness of Agulhas leakage was previously mentioned by Donners et al. (2004), who found that Agulhas leakage was limited to the upper 1200 m in their model. Furthermore, using observations, Van Aken et al. (2003) show that an Agulhas ring has low relative vorticity below 1200 m, which might imply that deeper than 1200 m there is almost no mass carried by the rings. In a model study, De Steur et al. (2004) showed that the size of the seperatrix (the circumference of the region where water is advected with an Agulhas ring) decreases with depth due to the decrease in swirl velocity of the water. At some depth, therefore, the swirl velocity is smaller than the translational velocity, and the Agulhas rings cannot advect water anymore (Flierl, 1981).

4. An optimum thermohaline threshold method

As already stated in the introduction, the goal of this study is to investigate how to relate the fluxes at the GoodHope line to the float-determined Agulhas leakage F_{AL}. The high agreement between the Eulerian and Lagrangian fluxes in Fig. 3 suggests that such a relation is feasible when only a subdomain of the GoodHope line is used. The first approach to determining the shape of this subdomain is based on the thermohaline properties of the Eulerian flux.

The change of the thermohaline characteristics of the water on its route through the Cape Basin can be assessed by comparing the temperature and salinity of the water where numerical floats cross the Agulhas Current retroflection (at 19°E) with the temperature and salinity of the water where numerical floats cross the GoodHope line (Fig. 5). At both sections there is a

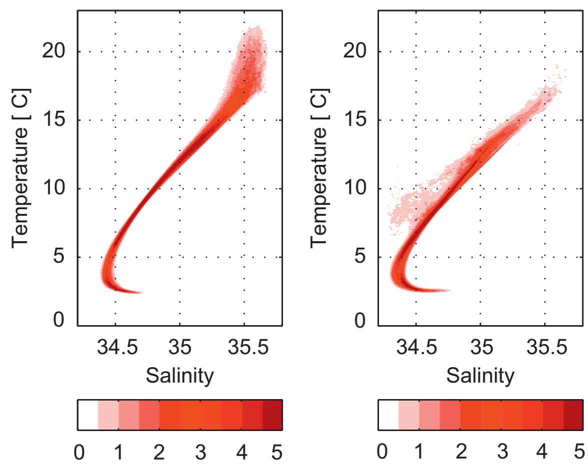

Fig. 5. The distribution of transport by the numerical Lagrangian floats as a function of temperature and salinity of the water at the location where the floats cross the 19°E section (left panel) and the GoodHope line (right panel), in 10^{-3} Sverdrup per $0.01\times0.05\,^{\circ}$C grid cell. A large fraction of the warm and saline thermocline water at the Agulhas Current retroflection has freshened and cooled on its path through the Cape Basin.

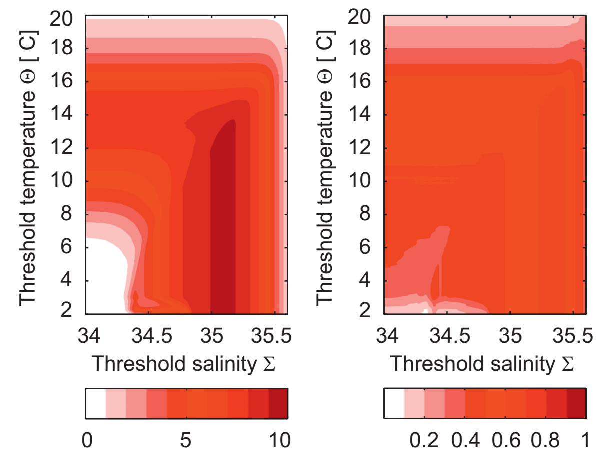

Fig. 6. The flux $F_{\Theta\Sigma}$ into the Atlantic Ocean over the GoodHope line when integration is done only over grid cells which are warmer and more saline than a certain threshold temperature Θ and threshold salinity Σ. The mean leakage as a function of these thresholds (left panel, in Sverdrup) and the correlation with the float-determined time series of Agulhas leakage time series as a function of these thresholds (right panel). The mean flux of Agulhas leakage is never above 10 Sv, which is considerably lower than the mean float-determined Agulhas leakage F_{AL}. The optimum thermohaline threshold values are these values Θ_0 and Σ_0 where the correlation is maximum.

significant amount of transport in cold and fresh subthermocline water and this transport appears to maintain its characteristics through the Cape Basin. Van Aken et al. (2003) already noted that below the 12 °C isotherm the water within Agulhas rings can not be distinguished from the surrounding water so that mixing does not alter the thermohaline characteristics of the Agulhas leakage. This suggests that integrating over water colder than 12 °C will probably introduce spurious fluxes and should be done with much precaution. The warm and saline thermocline water, on the other hand, is much fresher and colder when it crosses the GoodHope line. Apparently, this water has experienced atmospheric cooling and freshening and extensive mixing with the colder thermocline water of the Atlantic and Southern Oceans.

Although mixing appears to have a large impact on the Agulhas leakage as it crosses the GoodHope line, we can try to estimate the magnitude of Agulhas leakage in the model from the thermohaline properties of the flux at the GoodHope line. Assuming that Agulhas leakage is the warmest and most saline water at the GoodHope line, integration of the flux of water warmer than a certain threshold temperature Θ and more saline than a threshold salinity Σ might facilitate the discrimination between fluxes from the Indian Ocean and fluxes from the other two oceans. This Eulerian flux as a function of threshold temperature and threshold salinity can be written as

$$F_{\Theta\Sigma} = \int_{\theta=\Theta}^{\infty}\int_{\sigma=\Sigma}^{\infty} V(\theta,\sigma)\,d\sigma\,d\theta \quad (1)$$

where $V(\theta,\sigma)$ is the flux through all grid cells with temperature θ and salinity σ.

This method leads to fluxes $F_{\Theta\Sigma}$ as a function of threshold temperature, threshold salinity, and time (Fig. 6). For any combination of Θ and Σ, the method yields an underestimation of the mean magnitude of Agulhas leakage, as the mean flux never gets above 10 Sv and $F_{\Theta\Sigma}$ is even negative for low Θ and Σ. Integration is in that case then effectively over the whole GoodHope line, which apparently has a mean flux into the Indian Ocean (due to the eastward transport of the Antarctic Circumpolar Current).

The variability of the Eulerian time series, on the other hand, is much better captured by this method. The maximum correlation between the Eulerian and Lagrangian time series is 0.62, which is significantly different from zero at the 95% confidence level. This occurs for $\Theta_0 = 14.6\,^{\circ}$C and $\Sigma_0 = 35.33$. As we are mainly interested in capturing the variability of Agulhas leakage in an Eulerian estimate, these values represent the optimum thermohaline threshold values in this model. The mean Eulerian flux $F_{\Theta_0\Sigma_0}$ (7.7 Sv) is approximately half of the magnitude of the Lagrangian Agulhas leakage. This might be a reasonable estimate of the amount of Agulhas leakage in the thermocline, as it is close to the 9–10 Sv estimate of thermocline interocean exchange by Gordon et al. (1987) and Gordon et al. (1992).

Note that these optimum thermohaline threshold values do not necessarily have to mean that all water at the GoodHope line warmer than 14.6 °C and more saline than 35.33 is Agulhas leakage water; it only means that at Θ_0 and Σ_0 the correlation of the time series is largest. However, the greatest part of this warm and saline water in the model does seem to originate from the Agulhas Current. The transport by floats within water above these thresholds is 6.2 Sv, while the flux of all water above these thresholds is the aforementioned 7.7 Sv. This means that the warm and saline water at the GoodHope line is to a large extent 'pure' Agulhas leakage water.

The correlation between the magnitude of the float-determined Agulhas leakage and the Eulerian flux determined by this water mass analysis is relatively sensitive to Σ (Fig. 6). It is, however, not so sensitive to Θ. Apparently, at the GoodHope line in the model, water that is more saline than Σ_0 is generally also warmer than Θ_0 so the integration domain is controlled by the isohalines rather than the isotherms (Fig. 7). An explanation for this domination of salinity over temperature might be that the impact of the atmosphere on the temperature of the Agulhas leakage water is much higher than the impact on its salinity. On its journey through the Cape Basin, Agulhas leakage is more efficiently cooled than freshened. At the GoodHope line, therefore, the Agulhas leakage is probably better identified by its salinity than by its temperature.

Unfortunately, this domination of the salinity signal means that monitoring the magnitude of Agulhas leakage at the GoodHope line with only XBTs (expendable sensors which measure temperature as a function of depth) is not feasible. The optimum

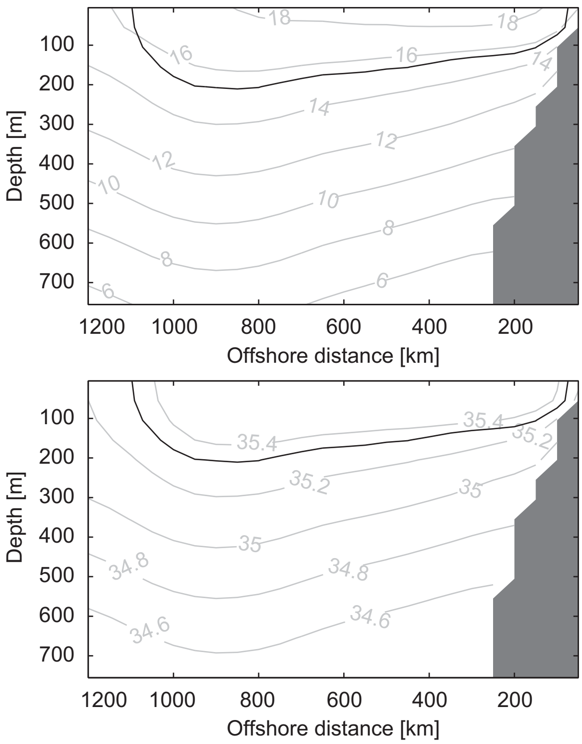

Fig. 7. The mean temperature (gray lines in the upper panel, in °C) and salinity (gray lines in the lower panel) in a subregion of the vertical plane at the GoodHope line over the 37 years integration period. The solid black lines indicate the mean of the sub-plane where the both temperature is above $\Theta_0 = 14.6\,^{\circ}\mathrm{C}$ and the salinity is above $\Sigma_0 = 35.33$, the threshold values where the correlation between $F_{\Theta\Sigma}$ and F_{AL} is highest. Note that this domain seems to follow isohalines rather than isotherms.

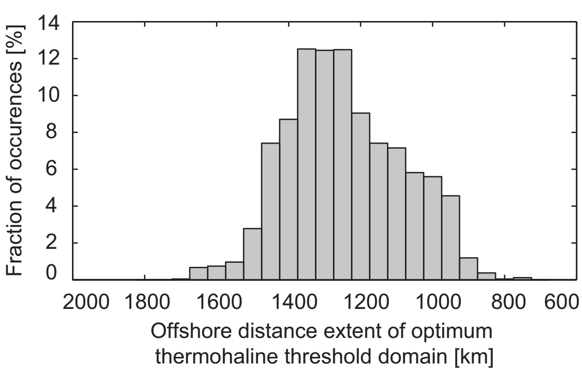

Fig. 8. The histogram of the offshore extent of the optimum thermohaline threshold domain. The offshore extent varies over time, and to always be able to capture it a CTD section should extent 1700 km offshore. At a 50 km horizontal spacing, this requires 34 CTD-casts or moorings.

thermohaline threshold domain appears to follow salinity much closer than temperature so that salinity information is indispensable (Fig. 7). A monitoring of $F_{\Theta_0\Sigma_0}$ would thus require either a mooring array equipped with CTDs or an extensive vessel-based CTD program. The optimum thermohaline threshold domain is maximally 500 m deep and 1700 km wide (Fig. 8). At the 50 km resolution used in this analysis, such a monitoring program would require in the order of 30 CTD stations or moorings.

Despite the underestimation of the magnitude of Agulhas leakage when the $\Theta_0 = 14.6\,^{\circ}\mathrm{C}$ and $\Sigma_0 = 35.33$ optimum thermohaline threshold values are used, the total magnitude of Agulhas leakage can be related to $F_{\Theta_0\Sigma_0}$ using a linear regression. In order

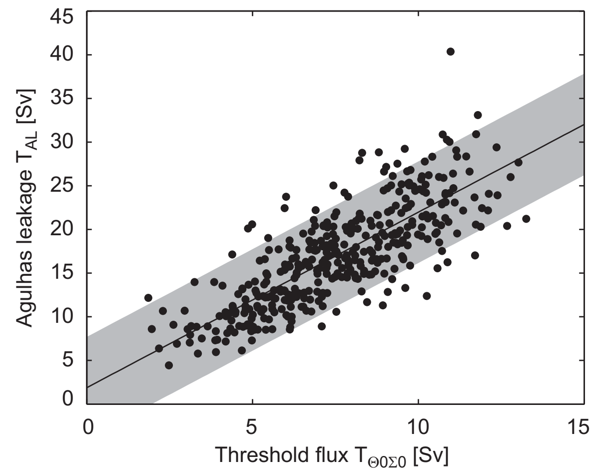

Fig. 9. The monthly binned float-determined Agulhas leakage transport T_{AL} versus the monthly binned Eulerian flux $T_{\Theta_0\Sigma_0}$ using the optimum thermohaline threshold values (dots), both at the GoodHope line. The correlation between the data sets is 0.80, which is significant at the 95% confidence level. The black line is the best linear fit and the gray area indicates the estimated confidence level so that 90% of the data points fall within the area. The confidence band width (the height of the gray area) is 11.6 Sv, and the slope of the best fit line is 2.0.

to reduce noise, the Eulerian and Lagrangian fluxes are binned to monthly values:

$$T_X(t) = \langle F_X(t) \rangle \tag{2}$$

where X is either AL or $\Theta\Sigma$ and $\langle \ldots \rangle$ is the 30 days binning operator.

The correlation between the smoothed float-determined transport T_{AL} and the smoothed threshold-determined flux $T_{\Theta_0\Sigma_0}$ is even larger than for the unsmoothed time series, at 0.80. The resulting linear regression can be used to form an estimate of the total magnitude of Agulhas leakage using the flux of warm ($\theta > \Theta_0$) and saline ($\sigma > \Sigma_0$) water:

$$E_{AL} = \alpha T_{\Theta_0\Sigma_0} + \beta \tag{3}$$

where the fitting parameters $\alpha = 2.0$ and $\beta = 1.9$ Sv are obtained from the best fit of the monthly means in Fig. 9.

The skill of this estimate can be quantified by assigning a confidence band to the linear estimate. As a first approximation, a confidence band (a constant offset from the best linear fit) is chosen such that 90% of the data points lie within the confidence band. Since the goal is to devise an optimal estimation strategy, the skill of the method is determined by how far an estimate is from the float-determined leakage and this is quantified by the confidence band.

The 90% confidence band results in an uncertainty of 11.6 Sv in the estimate. An estimate of the amount of Agulhas leakage based on flux through the optimum thermohaline threshold domain is therefore only certain within a 11.6 Sv range. This means that when $E_{AL} = 10.0$ Sv in the model, then the total flux of Agulhas leakage is with 90% confidence somewhere between 4.2 and 15.8 Sv.

It is also possible to devise an Eulerian estimate similar to that of Eq. (3) for the unsmoothed data set. However, the signal-to-noise level is then lower. Although the correlation between the two time series in that case is still significant, the 18.9 Sv confidence band is almost double as wide (not shown). This wide band limits the usability of the estimate. The advantage of the unsmoothed time series, however, is that it can more conveniently be measured using a vessel-based CTD program.

5. An optimum Euclidean integration method

Although it appears that within the model the magnitude of Agulhas leakage at the GoodHope line can to some extent be estimated using a linear regression, it might be somewhat disappointing that this Eulerian method can sample only half of the amount of Agulhas leakage directly. The high agreement between Eulerian and Lagrangian transport in the top-east part of the GoodHope line (Fig. 3) suggests that this fraction might be enhanced.

For this reason, a second and more straightforward approach to estimate the magnitude of Agulhas leakage in an Eulerian way is introduced. The method is based on limiting the integration domain to a rectangular subregion of the GoodHope line. Since the Eulerian and Lagrangian fluxes are so similar near the continent, we expect that one of the corners of this subregion must be located at the sea surface ($z=0$) at the African coast ($x=0$). The diametrically opposed corner is defined to be at depth Z and offshore distance X. This method yields an Eulerian flux time series F_{XZ}, which can be written in a way similar to $F_{\Theta\Sigma}$ in Eq. (1) as

$$F_{XZ} = \int_{x=0}^{X} \int_{z=0}^{Z} V(x,z)\,dz\,dx \tag{4}$$

where $V(x,z)$ is the flux through the grid cell at offshore distance x and depth z. Again, the goal is to find the X and Z where F_{XZ} is in best agreement with the time series of float-determined Agulhas leakage transport F_{AL}.

The mean of F_{XZ} is approximately equal to the mean of F_{AL} in a large U-shaped band between 700 km and 1500 km offshore (upper panel of Fig. 10). Closer to the coast, the Eulerian flux into the Atlantic Ocean is smaller than the mean of the float-determined time series, whereas farther offshore the eastward velocities in the Antarctic Circumpolar Current result in a negative mean of F_{XZ}. For large parts of the deep ocean, where the means of the Eulerian and Lagrangian fluxes are approximately equal, the variability in F_{XZ} is too large (middle panel of Fig. 10). This is related to the barotropic nature of the velocity profile at the GoodHope line in contrast to the more baroclinic float-determined Agulhas leakage transport (Fig. 3).

The optimum Euclidean integration area in the model is defined as the values X_0 and Z_0 where the root mean square difference between the Eulerian and Lagrangian time series is smallest. The root mean square distance is used as a measure instead of correlation because we want to directly measure the magnitude of Agulhas leakage and not estimate it through a linear regression. In the model the minimum root mean square distance (5.7 Sv) is located at $Z_0 = 300$ m and $X_0 = 900$ km (lower panel of Fig. 10). Note that the root mean square difference quickly increases for $Z > 300$ m but that the sensitivity with respect to X is smaller as long as the velocity integration is not extended into the Antarctic Circumpolar Current at $X = 1800$ km.

Similar to the approach followed in Eqs. (2) and (3), another Eulerian estimate E_{AL} can be constructed by using a 30 day binned averages of $F_{X_0Z_0}$. However, because X_0 and Z_0 are chosen such that almost all of the flux of Agulhas leakage is captured by integrating over the optimum Euclidean integration area, the parameters are fixed to $\alpha = 1$ and $\beta = 0$ Sv.

The correlation between the monthly binned float-determined Agulhas leakage transport T_{AL} and the integrated velocities $T_{X_0Z_0}$ is 0.49, which is significantly different from zero at the 95% confidence level (Fig. 11). Since this correlation is lower here than in the optimum thermohaline threshold method, the confidence band is almost twice as wide at 19.6 Sv. So although the mean Eulerian flux is closer to the float-determined Agulhas leakage transport when the optimum Euclidean integration method is used, the estimate constructed in this way is less skillful.

At horizontal and vertical resolutions of 50 km and 50 m, respectively, the optimum Euclidean integration area can be covered in the real ocean by 18 moorings carrying only an ADCP at the top. That is, of course, if the results from the Eulerian and Lagrangian fields in the AG01 model can be translated to the real

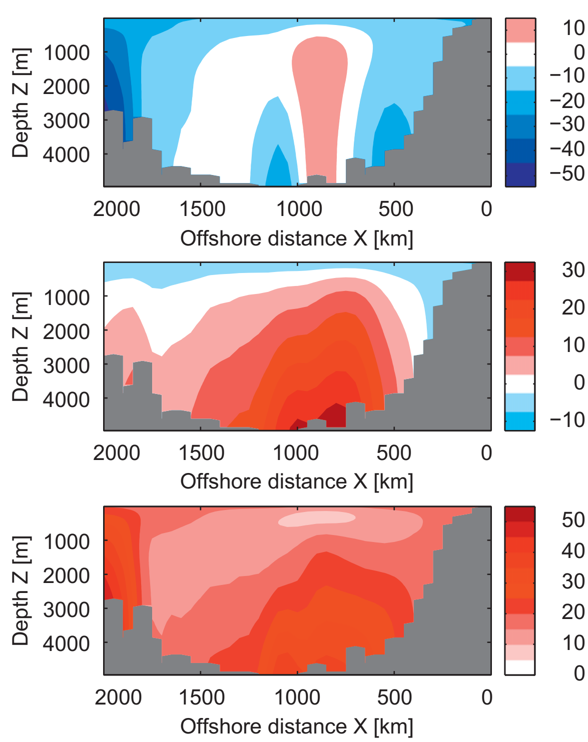

Fig. 10. Comparison of the Eulerian flux time series F_{XZ} and Lagrangian leakage time series F_{AL} at the GoodHope line. Integration starts at the sea surface at the African continent, and ends at a point (X,Z) on the vertical plane. For each of these points, the mean difference between the time series (upper panel), the difference of the standard deviations between the time series (middle panel), and the root mean square difference between the time series (lower panel) are shown in Sverdrup. The F_{XZ} time series is in best agreement with the F_{AL} time series for $X_0 = 300$ m and $Z_0 = 900$ km.

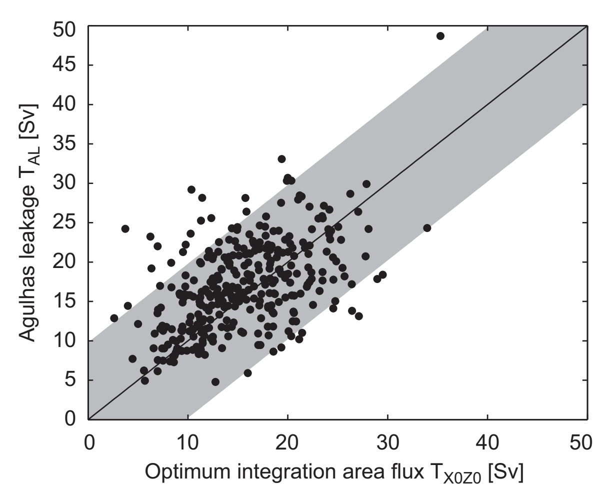

Fig. 11. The monthly binned float-determined Agulhas leakage transport T_{AL} versus the monthly binned Eulerian flux $T_{X_0Z_0}$ using the optimum Euclidean integration area (dots), both at the GoodHope line. The correlation between the data sets is 0.49, which is significant at the 95% confidence level. The black line is the one-to-one line, and the gray area denotes the 90% confidence band (of width 19.6 Sv), chosen such that 90% of the points fall within the gray area.

ocean. As the root mean square difference quickly increases when Z_0 is changed, application of this Eulerian method is sensitive to the details of the distribution of Agulhas leakage over the GoodHope line. As shown by Van Sebille et al. (2009b) the AG01 model does not perform extremely well at the GoodHope line. Although it cannot be concluded that the model has no skill at this location, the trajectories of the numerical floats in the upper 15 m are slightly too far offshore when compared to the trajectories of drifting buoys in the real ocean. This offshore model bias might translate in an offshore bias of the optimum Euclidean integration area, which will have implications for the constructed Agulhas leakage flux estimate.

6. Conclusions and discussion

An attempt has been made to devise an Eulerian measurement strategy for estimating the magnitude of Agulhas leakage in the real ocean. This has been done by relating the Eulerian (velocity-based) fluxes over the GoodHope line (Ansorge et al., 2005; Swart et al., 2008) to the 'true' (float-determined) time series of Agulhas leakage transport as obtained from numerical Lagrangian floats.

The difficulty with such an Eulerian method lies in posing the integration boundaries. An optimum has to be found between a too small integration domain (which does not capture all Agulhas leakage transport) and a too large domain (which introduces spurious fluxes from other sources than the Indian Ocean). Two methods for finding the optimum integration boundaries have been tested. In the first method, integration is limited to a subdomain of thermohaline (temperature–salinity) space. Since Indian Ocean water is generally warmer and more saline than Atlantic Ocean and Southern Ocean water, integration of velocities is limited to grid cells where the water is warmer and more saline than the optimum thermohaline threshold values $\Theta_0 = 14.6\,^{\circ}\mathrm{C}$ and $\Sigma_0 = 35.33$. The time series obtained in this way has an 0.62 correlation with the 'true' Agulhas leakage transport time series. In the model, these water masses extend until at most 1700 km offshore so that it requires more than 30 CTD profiles at 50 km spacing to completely capture the flux.

Another way to find the optimum integration boundaries is by optimizing the time series in Euclidean (offshore distance–depth) space. In this method, the velocity is only integrated over a subregion of the vertical plane at the GoodHope line. The method yields an empirically determined optimum Euclidean integration area, an area where the root mean square distance between the float-determined Agulhas leakage transport and the velocity-integrated flux is smallest. This is the case when integration is confined to water shallower than $Z_0 = 300$ m and closer to the coast than $X_0 = 900$ km. The time series this yields has an 0.49 correlation with the 'true' Agulhas leakage transport time series. At the resolution used for this analysis, the area can be covered in the real ocean by an array of 18 ADCPs.

Although this second method works well in this model, it is unsure what its skill is in other models or in the real ocean. The shape of the optimum Euclidean integration area will depend on the details of the circulation in the Cape Basin, which are reasonably resolved in the model (Biastoch et al., 2008c; Van Sebille et al., 2009b). Since the skill of the optimum Euclidean integration method quickly deteriorates when the area of integration is changed, this method requires calibration by an independently obtained time series of Agulhas leakage transport. The best way to obtain such an independent time series of Agulhas leakage transport is by performing a Lagrangian experiment. However, the costs of deploying millions of floats is so high that this is unfeasible in the real ocean.

In principle this calibration problem also holds for the thermohaline method, but we expect that it is not as important. The thermohaline method depends not on the details of the local circulation in the Cape Basin, but on the temperature and salinity characteristics of the different oceans. These large-scale patterns are probably better resolved in the model than the small-scale eddy field and therefore we have more confidence in the universality of Θ_0 and Σ_0 than in the universality of X_0 and Z_0.

The thermohaline method leads to a mean Eulerian flux $F_{\Theta_0\Sigma_0}$ which is only half of the mean float-determined Agulhas leakage transport F_{AL}, although the time series of F_{AL} and $F_{\Theta_0\Sigma_0}$ are highly correlated. The mean Eulerian flux based on the optimum Euclidean integration area $F_{X_0Z_0}$, on the other hand, is only a few Sverdrups lower than the mean of F_{AL}. Nevertheless, the thermohaline method leads to a more skillful estimate E_{AL} of the monthly mean magnitude of Agulhas leakage than the optimum Euclidean integration method, with confidence bands of 11.6 Sv and 19.6 Sv, respectively. This is probably because the first method is based on the well-established water mass analysis, whereas the second method is purely empiric.

One last remark: As already noted in Section 2, there seems to be a discrepancy in the use of Lagrangian floats is this study. On the one hand, the floats are treated as point particles which are passively advected within the model circulation. The floats are advected with the flow and can move into areas of different temperature and salinity. On the other hand the floats have a transport, approximately 0.1 Sv, which is used to assess the magnitude of Agulhas leakage. Finite-volume floats can only change their thermohaline properties if they are allowed to mix the water they carry with the ambient water. But if the transport by a float is mixed on its route to the Atlantic Ocean it will get diluted and its transport as it crosses the GoodHope line is not pure Agulhas Current water anymore, as is required by the definition of Agulhas leakage.

However, this is not a real contradiction. The point is that the floats do not *carry* transport, but that they *represent* transport. As such, they are point particles which have no volume and therefore also lack thermohaline properties. The Agulhas Current is sampled according to its transport when the floats are released. The float-determined Agulhas leakage transport is thus a statistical quantity rather than a deterministic quantity. The accuracy of F_{AL} will increase when more floats are released so that each represents a smaller transport. As a typical float in this study represents only $2.2\times10^{-5}\%$ of the total volume transport by all floats, we can assume that F_{AL} is reasonably accurate. Thus, the apparent dichotomy is not real.

All in all, this study indicates that it may be feasible to make a reasonably accurate estimate of the magnitude of Agulhas leakage at monthly resolution. This can be achieved by deploying a mooring array at the GoodHope line, where temperature, salinity, and velocity are measured within the thermocline. Something like the TOGA-TAO array (Hayes et al., 1991), but in the Agulhas region rather than the equatorial Pacific Ocean.

Acknowledgments

EvS is sponsored by the SRON User Support Programme under Grant EO-079, with financial support from the Netherlands Organization for Scientific Research, NWO. PJvL is partly supported by the MERSEA project of the European Commission under Contract SIP3-CT-2003-502885. Model and float integrations have been performed at the Höchstleistungsrechenzentrum Stuttgart (HLRS). The AVISO data set was produced by Ssalto/Duacs, with support from CNES.

References

Ansorge, I.J., Speich, S., Lutjeharms, J.R.E., Goni, G.J., Rautenbach, C.J., Froneman, P.W., Rouault, M., Garzoli, S.L., 2005. Monitoring the oceanic flow between Africa and Antarctica: report of the first GoodHope cruise. S. African J. Sci. 101, 29–35.

Baker-Yeboah, S., 2008. Sea surface height variability and the structure of eddies in the South Atlantic Cape Basin. Ph.D. Thesis, University of Rhode Island.

Bang, N.D., Andrews, W.R.H., 1974. Direct current measurements of a shelf-edge frontal jet in the southern Benguela system. J. Mar. Res. 32, 405–417.

Biastoch, A., Beal, L.M., Lutjeharms, J.R.E., Casal, T.G.D., 2009a. Variability and coherence of the Agulhas Undercurrent in a high-resolution ocean general circulation model. J. Phys. Oceanogr. 39, 2417–2435.

Biastoch, A., Böning, C.W., Schwarzkopf, F.U., Lutjeharms, J.R.E., 2009b. Increase in Agulhas leakage due to poleward shift of Southern Hemisphere westerlies. Nature 462, 495–499.

Biastoch, A., Böning, C.W., Getzlaff, J., Molines, J.-M., Madec, G., 2008a. Causes of interannual-decadal variability in the Meridional Overturning Circulation of the midlatitude North Atlantic Ocean. J. Clim. 21, 6599–6615.

Biastoch, A., Böning, C.W., Lutjeharms, J.R.E., 2008b. Agulhas leakage dynamics affects decadal variability in Atlantic overturning circulation. Nature 456, 489–492.

Biastoch, A., Lutjeharms, J.R.E., Böning, C.W., Scheinert, M., 2008c. Mesoscale perturbations control inter-ocean exchange south of Africa. Geophys. Res. Lett. 35, L20602.

Blanke, B., Raynaud, S., 1997. Kinematics of the Pacific Equatorial undercurrent: an Eulerian and Lagrangian approach from GCM results. J. Phys. Oceanogr. 27, 1038–1053.

Boebel, O., Lutjeharms, J.R.E., Schmid, C., Zenk, W., Rossby, T., Barron, C.N., 2003. The Cape Cauldron, a regime of turbulent inter-ocean exchange. Deep-Sea Res. II 50, 57–86.

Bryden, H.L., Beal, L.M., Duncan, L.M., 2005. Structure and transport of the Agulhas Current and its temporal variability. J. Oceanogr. 61, 479–492.

Byrne, D.A., Gordon, A.L., Haxby, W.F., 1995. Agulhas Eddies: a synoptic view using Geosat ERM data. J. Phys. Oceanogr. 25, 902–917.

Byrne, D.A., McClean, J.L., 2008. Sea level anomaly signals in the Agulhas Current region. Geophys. Res. Lett. 35, L13601.

Casal, T.G.D., Beal, L.M., Lumpkin, R., Johns, W.E., 2009. Structure and downstream evolution of the Agulhas Current system during a quasi-synoptic survey in February–March 2003. J. Geophys. Res. 114, C03001.

De Steur, L., Van Leeuwen, P.J., Drijfhout, S.S., 2004. Tracer leakage from modeled Agulhas rings. J. Phys. Oceanogr. 34, 1387–1399.

Debreu, L., Vouland, C., Blayo, E., 2008. AGRIF: adaptive grid refinement in Fortran. Comput. Geosci. 34, 8–13.

Dijkstra, H.A., De Ruijter, W.P.M., 2001. On the physics of the Agulhas current: steady retroflection regimes. J. Phys. Oceanogr. 31, 2971–2985.

Doglioli, A.M., Veneziani, M., Blanke, B., Speich, S., Griffa, A., 2006. A Lagrangian analysis of the Indian–Atlantic interocean exchange in a regional model. Geophys. Res. Lett. 33, L14611.

Donners, J., Drijfhout, S.S., 2004. The lagrangian view of South Atlantic interocean exchange in a global ocean model compared with inverse model results. J. Phys. Oceanogr. 34, 1019–1035.

Donners, J., Drijfhout, S.S., Coward, A.C., 2004. Impact of cooling on the water mass exchange of Agulhas rings in a high resolution ocean model. Geophys. Res. Lett. 31, L16312.

Flierl, G.A., 1981. Particle motions in large-amplitude wave fields. Geophys. Astrophys. Fluid Dyn. 18, 39–74.

Ganachaud, A., Wunsch, C., 2000. Improved estimates of global ocean circulation, heat transport, and mixing from hydrographic data. Nature 408, 453–456.

Garzoli, S.L., Goni, G.J., 2000. Combining altimeter observations and oceanographic data for ocean circulations and climate studies. Elsevier Oceanographic Series, pp. 79–97 (Chapter 5).

Giulivi, C.F., Gordon, A.L., 2006. Isopycnal displacements within the Cape Basin thermocline as revealed by the Hydrographic Data Archive. Deep-Sea Res. I 53, 1285–1300.

Gordon, A.L., 1986. Interocean exchange of thermocline water. J. Geophys. Res. 91, 5037–5046.

Gordon, A.L., Bosley, K.T., Aikman III, F., 1995. Tropical Atlantic water within the Benguela upwelling system at 27°S. Deep-Sea Res. I 42, 1–12.

Gordon, A.L., Lutjeharms, J.R.E., Gründlingh, M.L., 1987. Stratification and circulation at the Agulhas Retroflection. Deep-Sea Res. A 4, 565–599.

Gordon, A.L., Susanto, R.S., Ffield, A., 1999. Throughflow within Makassar Strait. Geophys. Res. Lett. 26, 3325–3328.

Gordon, A.L., Weiss, R.F., Smethie Jr., W.M., Warner, M.J., 1992. Thermocline and intermediate water communication between the South Atlantic and Indian Oceans. J. Geophys. Res. 97, 7223–7240.

Hayes, S.P., Mangum, L.J., Picaut, J., Sumi, A., Takeuchi, K., 1991. TOGA-TAO: a moored array for real-time measurements in the tropical Pacific Ocean. Bull. Am. Meteorol. Soc. 72, 339–347.

Hermes, J.C., Reason, C.J.C., Lutjeharms, J.R.E., 2007. Modeling the variability of the Greater Agulhas Current System. J. Clim. 20, 3131–3146.

Knorr, G., Lohmann, G., 2003. Southern Ocean origin for the resumption of Atlantic thermohaline circulation during deglaciation. Nature 424, 532–536.

Large, W.G., Yeager, S.G., 2004. Diurnal to decadal global forcing for ocean and sea-ice models: the data sets and flux climatologies. NCAR Technical Note NCAR/TN-460+STR, NCAR.

Lutjeharms, J.R.E., Cooper, J., 1996. Interbasin leakage through Agulhas Current filaments. Deep-Sea Res. I 43, 213–238.

Madec, G., 2006. NEMO ocean engine. Note du pôle de modélisation, Institut Pierre-Simon Laplace (IPSL).

Matano, R.P., Beier, E.J., 2003. A kinematic analysis of the Indian/Atlantic inter-ocean exchange. Deep-Sea Res. II 50, 229–250.

Reason, C.J.C., Lutjeharms, J.R.E., Hermes, J., Biastoch, A., Roman, R.E., 2003. Inter-ocean fluxes south of Africa in an eddy-permitting model. Deep-Sea Res. II 50, 281–298.

Richardson, P.L., 2007. Agulhas leakage into the Atlantic estimated with subsurface floats and surface drifters. Deep-Sea Res. I 54, 1361–1389.

Ridderinkhof, H., Van der Werf, P.M., Ullgren, J.E., Van Aken, H.M., Van Leeuwen, P.J., De Ruijter, W.P.M., 2010. Seasonal and interannual variability in the Mozambique Channel from moored current observations. J. Geophys. Res., in press.

Schmitz Jr, W.J., 1995. On the interbasin-scale thermohaline circulation. Rev. Geophys. 33, 151–173.

Schouten, M.W., De Ruijter, W.P.M., Van Leeuwen, P.J., Lutjeharms, J.R.E., 2000. Translation, decay and splitting of Agulhas rings in the southeastern Atlantic Ocean. J. Geophys. Res. 105, 21913–21925.

Speich, S., Lutjeharms, J.R.E., Penven, P., Blanke, B., 2006. Role of bathymetry in Agulhas Current configuration and behaviour. Geophys. Res. Lett. 33, L23611.

Swart, S., Speich, S., Ansorge, I.J., Goni, G.J., Gladyshev, S., Lutjeharms, J.R.E., 2008. Transport and variability of the Antarctic Circumpolar Current South of Africa. J. Geophys. Res. 113, C09014.

Thompson, S.R., Stevens, D.P., Döös, K., 1997. The importance of interocean exchange South of Africa in a numerical model. J. Geophys. Res. 102, 3303–3315.

Treguier, A.M., Boebel, O., Barnier, C., Madec, G., 2003. Agulhas eddy fluxes in a 1/6° Atlantic model. Deep-Sea Res. II 50, 251–280.

Van Aken, H.M., Van Veldhoven, A.K., Veth, C., De Ruijter, W.P.M., Van Leeuwen, P.J., Drijfhout, S.S., Whittle, C.C., Rouault, M., 2003. Observations of a young Agulhas ring, Astrid, during MARE in March 2000. Deep-Sea Res. II 50, 167–195.

Van Sebille, E., Barron, C.N., Biastoch, A., Van Leeuwen, P.J., Vossepoel, F.C., De Ruijter, W.P.M., 2009a. Relating Agulhas leakage to the Agulhas Current retroflection location. Ocean Sci. 5, 511–521.

Van Sebille, E., Van Leeuwen, P.J., Biastoch, A., Barron, C.N., De Ruijter, W.P.M., 2009b. Lagrangian validation of numerical drifter trajectories using drifting buoys: application to the Agulhas region. Ocean Model. 29, 269–276.

Van Sebille, E., Van Leeuwen, P.J., Biastoch, A., De Ruijter, W.P.M., 2010. On the fast decay of Agulhas rings. J. Geophys. Res., in press.

Weijer, W., De Ruijter, W.P.M., Dijkstra, H.A., Van Leeuwen, P.J., 1999. Impact of interbasin exchange on the Atlantic overturning circulation. J. Phys. Oceanogr. 29, 2266–2284.

You, Y., Lutjeharms, J.R.E., Boebel, O., De Ruijter, W.P.M., 2003. Quantification of the interocean exchange of intermediate water masses around southern Africa. Deep-Sea Res. II 50, 197–228.